Metallophysics and Advanced Technologies
Металофіз. новітні технол.
Metallofiz. Noveishie Tekhnol.
2023, vol. 45, No. 8, pp. 951–961
https://doi.org/10.15407/mfint.45.08.0951
Reprints available directly from the publisher

PACS numbers: 61.66.Dk, 65.40.De, 81.20.Ev, 81.20.Wk, 81.40.Cd, 81.40.Vw, 81.70.Pg

Sintered Al–Si–Ni Alloy: Structure and Properties. I. Powder Obtaining

G. A. Bagliuk, T. O. Monastyrska*, V. V. Kaverinsky, V. P. Bevz*, V. K. Nosenko*, I. M. Kirian*, D. L. Pakula*, V. V. Kyrylchuk*, A. M. Lakhnik*, and O. D. Rud*

I. M. Frantsevych Institute for Problems in Materials Science, N.A.S. of Ukraine,
3 Omeljan Pritsak Str.,
UA-03142 Kyiv, Ukraine
**G. V. Kurdyumov Institute for Metal Physics, N.A.S. of Ukraine,*
36 Academician Vernadsky Blvd.,
UA-03142 Kyiv, Ukraine

The work is aimed at the development of a new sintered aluminium alloy with a low temperature coefficient of linear expansion that opens fundamentally new opportunities for solving the modern needs of domestic machine-building and instrument-making enterprises in light materials with special physical properties. Phase composition, structure and properties of cast aluminium alloys Al–Si–Ni with different contents of silicon and nickel, as well as powders obtained by grinding rapidly-quenched metal ribbons of these alloys in a high-energy ball mill are studied using various methods of structural analysis. The obtained values of the coefficient of linear expansion of the studied alloys in the cast state are significantly lower than those of pure aluminium, and they amount to $\cong (11–15)\cdot 10^{-6}\ \mathrm{K}^{-1}$. The method of obtaining a powder of a rapidly-crystallized alloy by manufacturing a rapidly-quenched metal ribbons using melt spinning followed by its dispersion in a high-energy ball mill is proposed for the fabrication of finely-dispersed powder and subsequent hot pressing.

Key words: sintered aluminium alloy, Al–Si–Ni, powder metallurgy, compaction, alloying, melt spinning, rapidly-quenched ribbons, coefficient of linear expansion.

Corresponding author: Oleksandr Dmytrovych Rud
E-mail: rud@imp.kiev.ua

Citation: G. A. Bagliuk, T. O. Monastyrska, V. V. Kaverinsky, V. P. Bevz, V. K. Nosenko, I. M. Kirian, D. L. Pakula, V. V. Kyrylchuk, A. M. Lakhnik*, and O. D. Rud, Sintered Al–Si–Ni Alloy: Structure and Properties. I. Powder Obtaining, *Metallofiz. Noveishie Tekhnol.*, **45**, No. 8: 951–961 (2023). DOI: 10.15407/mfint.45.08.0951

Роботу спрямовано на розробку нового спеченого алюмінійового стопу з низьким температурним коефіцієнтом лінійного розширення, що відкриває принципово нові можливості вирішення сучасних потреб вітчизняних підприємств машинобудування, приладобудування у легких матеріялах з особливими фізичними властивостями. З використанням різних методів структурної аналізи вивчено фазовий склад, структуру та властивості литих алюмінійових стопів Al–Si–Ni з різним вмістом Силіцію та Ніклю, а також порошків, одержаних розмелюванням у високоенергетичному кульовому млині швидкозагартованих металевих стрічок цих стопів. Одержані значення коефіцієнта лінійного розширення досліджених стопів у литому стані істотно нижчі, ніж у чистого алюмінію, і становлять $\cong (11–15)\cdot 10^{-6}$ К$^{-1}$. Запропоновано метод одержання порошку швидкозакристалізованого стопу шляхом виготовлення швидкозагартованої металевої стрічки за допомогою спінінґування розтопу з подальшим її дисперґуванням у високоенергетичному кульовому млині для одержання дрібнодисперсного порошку та наступного гарячого пресування.

Ключові слова: спечений алюмінійовий стоп, Al–Si–Ni, порошкова металурґія, компактування, леґування, спінінґування, швидкозагартовані стрічки, коефіцієнт лінійного розширення.

(Received August 9, 2023; in final version, August 11, 2023)

1. INTRODUCTION

The field of device construction, in particular the creation of aerospace equipment, requires lightweight materials with specific physical properties [1, 2]. One such property is the coefficient of thermal expansion (CTE) consistent with other materials they are in contact with, such as steel, copper alloys, *etc*. In particular, this parameter is crucial for flying object orientation and navigation devices. The error in determining the coordinates of navigation sources due to the part's dimensions instability could be up to 20–50% of the total error of the device [3]. Thus, the light materials design with a low CTE for special instrumentation of the aerospace complex is one of the urgent problems of modern metallurgy and materials science.

The basis of many lightweight materials is aluminium, which is not surprising because of its undeniable advantages: low density (2700 kg/m^3), high corrosion resistance and elasticity. Furthermore, it is relatively inexpensive, not toxic, malleable, and technological in processing [4], especially compared with other light metals and alloys based on magnesium, beryllium, or lithium. However, one of aluminium's disadvantages is its high coefficient of linear thermal expansion, which is $23.4\cdot 10^{-6}$ K^{-1} in the temperature range of 20–100°C [5]. For example, for steels it is $\cong (11–15)\cdot 10^{-6}$ K^{-1} [6] and $16.8\cdot 10^{-6}$ K^{-1} [7] for copper, respectively. Thus, it is crucial to reduce CTE for aluminium-based instrument-making materials. It could be achieved mainly

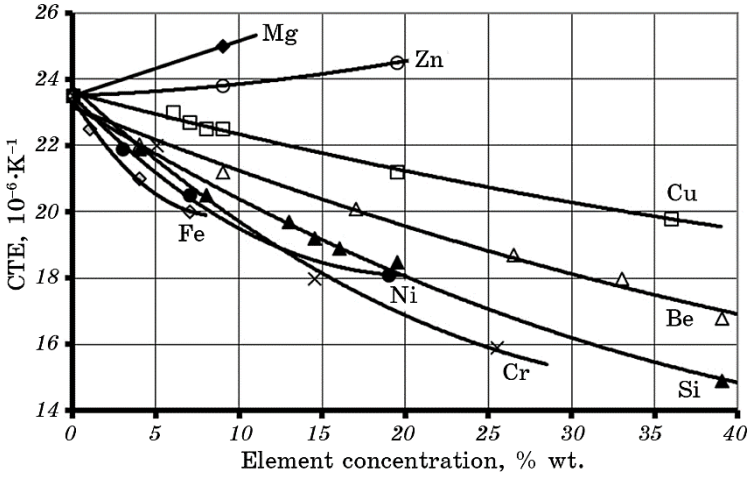

Fig. 1. Influence of alloying elements on CTE of aluminium alloys [4].

through special alloying.

In Figure 1, plots based on data from Ref. [4] are given and demonstrate the influence of the main alloying components used for aluminium on the materials' CTE.

It could be seen from the plots, Cr, Si, Be, and Cu reduce the CTE of aluminium, but Zn and Mg increase it. The primary attention should be given to Si. It is not only a popular doping element for aluminium alloys and could be used in a significant amount; moreover, it has a density even lower than Al, which means that its additive does not make the alloy any heavier. However, increasing its content by more than 30–35% is strongly not recommended because of the markedly reduced mechanical properties. Thereby, an additional alloying with other elements is needed. Such elements could be Cr, Ni, and Fe. Among them, Cr has a more significant influence in its high amounts. Fe is usually considered a not beneficial impurity, and the properties will be lower than when Ni is used. Ni has an appropriate impact on CTE in relatively low amounts. Thus, the final choice has fallen to the Al–Si–Ni system. The alloying components' contents are 25–35% of Si and 5–7% of Ni.

The main technological challenge during such material manufacture is to produce a homogenous product with appropriate structure and properties. In this case, it is strictly not recommended to use casting products as it usually could be done for ordinary Al–Si alloys (silumin). The main reason is its wide range of solidification temperatures. From the phase diagram shown in Fig. 2, it can be seen that for the alloy with 30% Si liquidus temperature is about 850°C, but the solidus temperature is 557°C. The phases present at this temperature interval are Si and intermetallic compounds, which are brittle and tend to grow

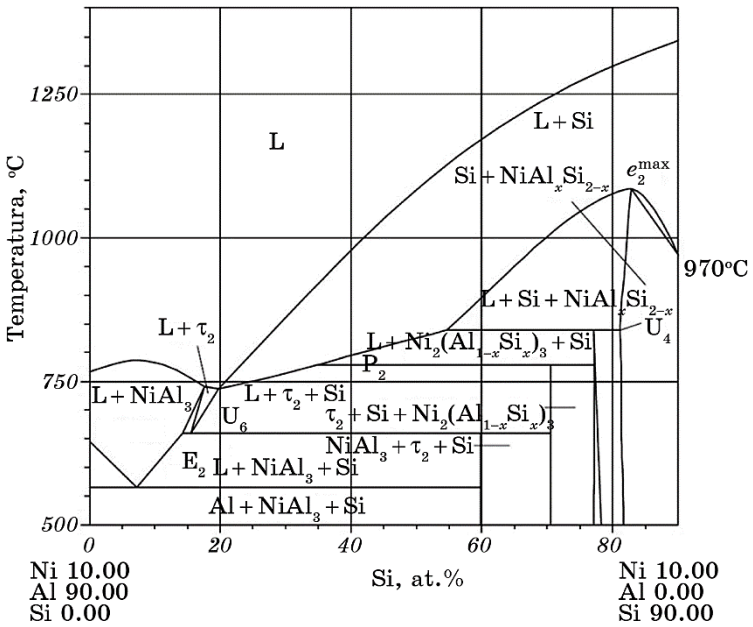

Fig. 2. A polythermal section of the Al–Si–Ni phase diagram for a Ni content of 10% [8].

being placed in a liquid-phase solution. Furthermore, such alloy is likely to liquate because of the density distinction between phases.

Isothermal sections of the corresponding ternary diagram could be found in works [9, 10] for temperatures 550, 750, and 850°C. It can be seen from those diagrams that at a temperature of 550°C, the range of compositions corresponding to the considered alloy corresponds to the zone of three-phase equilibrium (Al)–Si–$NiAl_3$. There is no liquid phase in the equilibrium state for the conditions. At the temperature of 750°C, the liquid phase is present at this region of the phase diagram. The more quantity of the liquid phase, the less silicon contains in the system. The other equilibrium phases at this temperature are Si, and the ternary intermetallic compound is marked as τ_3. At a temperature of 850°C, the composition range corresponding to the alloy belongs to the liquid phase zone on the state diagram. This one means that the material will completely melt at this temperature. However, the oxide frame inherent to the aluminium powder-made materials will probably allow keeping the form of the product even during liquid phase presence.

For the mentioned reasons, the high limit of Si content for cast Al–Si alloys is about 20–23% [11]. Therefore, powder metallurgy is the only appropriate method that could be applied for such a material production. Thus, the first primary task to appear is a production of a pre-

alloyed powder of the given composition for the usage of elemental components powders mixture does not seem to be a good idea because of the lower sinterability, porosity, and rough structure of the material obtained in such a way. Taking into account the problems mentioned above in a cast product of the desired composition manufacture, the production of the pre-alloyed powder turns into a challenge that needs a complex study for its solution.

The principal purpose of the part of the study presented here is the development of the fabrication technique of the Al–Si–Ni pre-alloyed powder, which contains ≅ 25–30% Ni and 5–7% Ni useful for subsequent sintered material manufacture.

2. RESEARCH MATERIAL AND METHODOLOGY

The experimental alloys were obtained in the shape of rapidly quenched ribbons. The ribbon thickness was in the range of 30–50 μm. The strips were obtained by spinning them on a rotating copper disk. The entire process control was provided in terms of the melt temperature, the pressure value in the crucible with the melt, and the barrel rotation speed. The initial materials were melted in the quartz crucibles. The strips were produced in a sealed chamber under a protective helium atmosphere. The linear disk surface speed was of 50 m/s, and the melt temperature was of 1080°C.

The chemical compositions and the strips' cross-sections dimensions are presented in Table 1.

The alloy powder was produced by the mechanical grinding of the original ribbons in a Fritsch Pulverisette P-6 planetary ball mill in a stainless steel bowl. The total duration of grinding was of 30 min. The number of steel balls with a diameter of 20 mm was of 12, and the mass

TABLE 1. Chemical composition of the alloys and the ribbon cross-section dimensions.

Material form	Chemical composition, % wt.				Ribbon cross-sections dimensions	
	Al	Si	Ni	Fe	Width d, mm	Thickness t, μm
Alloy 1		23.61	4.73	0.05		
Alloy 2		27.73	4.68	0.05	–	
Alloy 3		19.48	6.13	0.05		
Ribbon 1	base	26.5	6.95	0.05	9	30–40
Alloy 4		25.45	5.94	0.05		
Alloy 5		25.58	5.88	0.05	–	
Ribbon 2		25.58	5.88	0.05	12	30–40

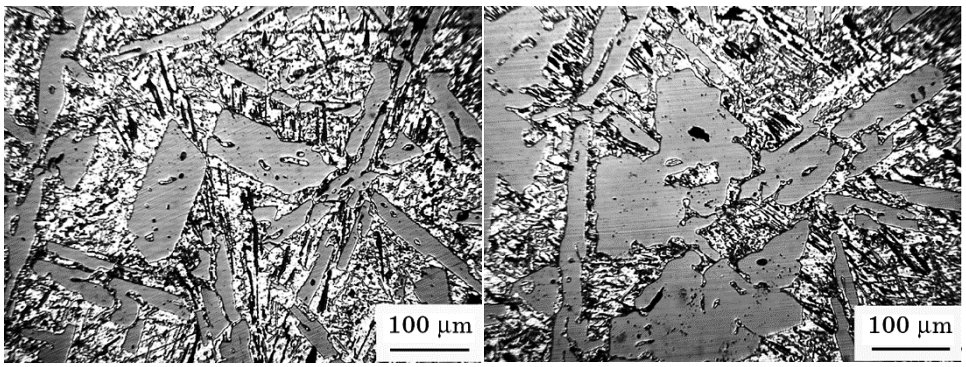

Fig. 3. Microstructure of the initial cast alloy: ingot top (*a*), ingot bottom (*b*).

of the powder was of ≅ 37 g. The milling speed and ball-to-powder mass ratio m_b:m_p were 200 rpm and 10:1, respectively. The specified synthesis conditions were applied to all the samples.

Dilatometric measurements were carried out using a dilatometer with an inductive transducer. The error of CTE estimation on the final experimental curves was of $\pm 0.3 \cdot 10^{-6}$ K^{-1}. Calorimetric analysis was performed on a DSC 404 F1 Pegasus® instrument (NETZSCH) in dynamic mode at a heating rate of 20 K/s in the temperature range from 20 to 700°C. The phase composition study of the alloys was carried out on a DRON-4 diffractometer using radiation CuK_α. Metallographic

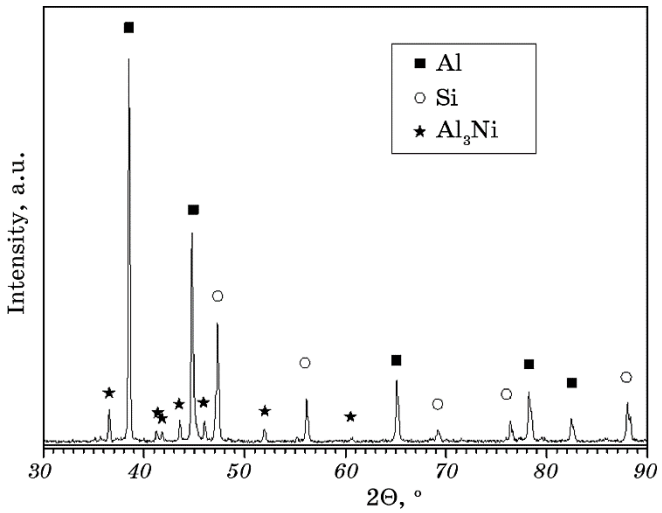

Fig. 4. X-ray pattern of the initial alloy obtained by crystallization with a cooling rate of 10^2 K/s.

studies were carried out on a NEOPHOT-2 optical microscope. A solution of 0.5 ml of HF in water was used to identify structural features.

3. RESEARCH RESULTS AND DISCUSSION

The typical microstructure of the initial alloys (used for subsequent quick-quenched ribbons obtaining) is presented in Fig. 3. The overall look of the structure given corresponds to a hypereutectic Al–Si alloy (so-called 'silumin'). Large-size fragile primary silicon crystals, which are peculiar to it, are up to 300 μm in size. The matrix is a ternary eutectic structure containing the α-solid solution of Si in Al (close to pure aluminium), Si, and intermetallic Al_3Ni particles. Primary silicon crystals have the form of equiaxed polyhedra with different numbers of faces. The observed structure causes low elasticity and a limited deformation processing possibility [11].

The structural difference between various parts of the ingot (Fig. 3) is clear evidence of the mentioned above volumetric liquation to which such alloys tend.

The phase composition of the initial alloys was also confirmed through x-ray diffraction (Fig. 4). The phase composition seems to be equilibrium. Non-equilibrium intermetallic compounds and silicides are not found. There are reasons to believe that such phase composition will also be in the sintered products after the solid phase sintering.

Metallographic studies obtained by the spinning method ribbons showed the presence of two zones with different etch abilities (Fig. 5, *a*): 1) a homogeneous structure on the contact side adjacent to the barrel (with 15–20 μm thickness), 2) a columnar structure with features

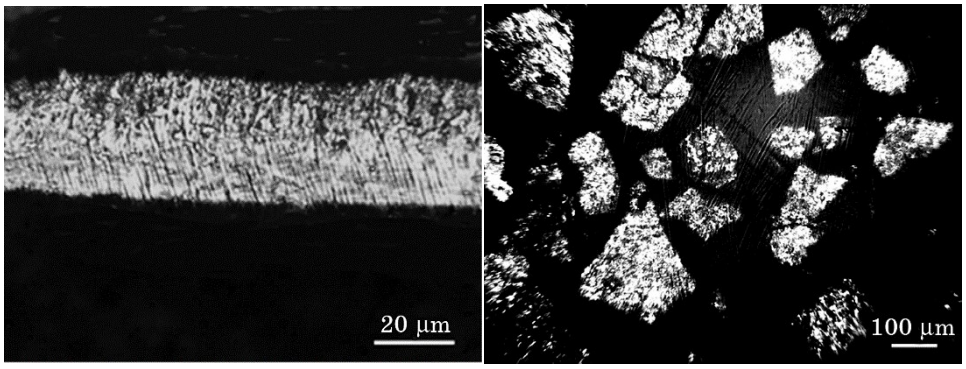

a *b*

Fig. 5. The cross-sectional structure of the rapidly-quenched ribbon (*a*) and the powder particle shape produced by ball milling of the strips within 30 minutes (*b*).

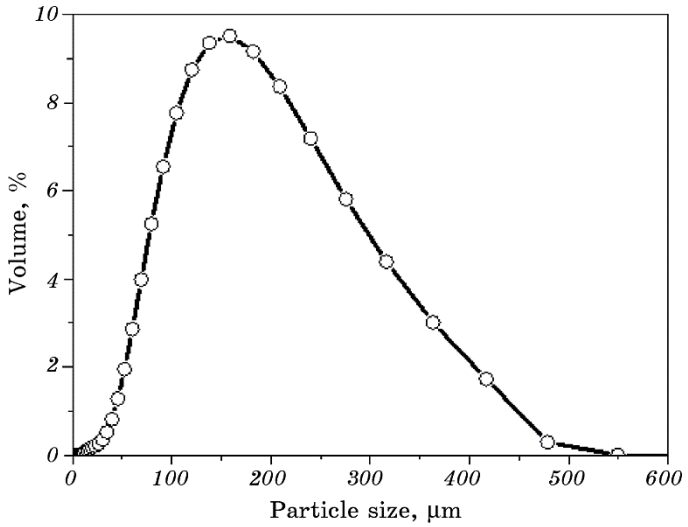

Fig. 6. The powder particles size distribution curve.

of fibrousness on the free side of the ribbon.

Since the ribbons of the alloy are obtained at high crystallization rates (10^5–10^6 K/s), their structure differs significantly from the equilibrium one. Primary silicon crystals in the ribbon structure cannot be detected under the optical microscope magnification.

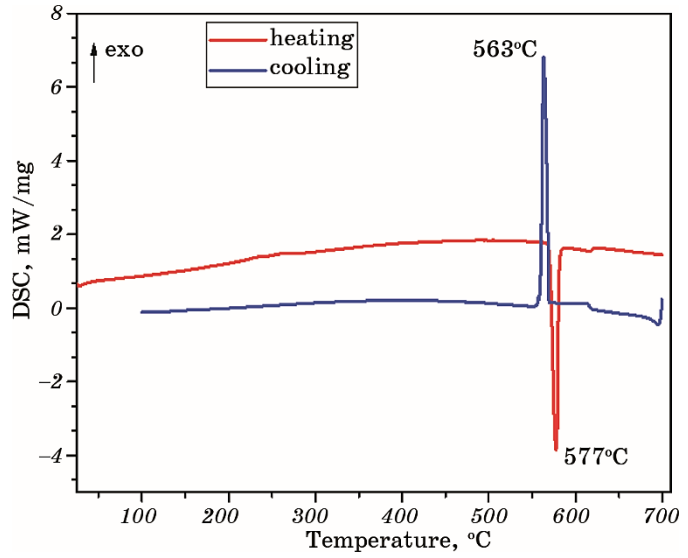

Fig. 7. Typical DSC heating–cooling curves of the alloy powder.

The alloy powder was manufactured by grinding the quick-hardened metal ribbons in a high-energy ball mill. The powder was produced by grinding the original rapidly-quenched metal ribbons into 300–400 μm particles.

Figure 5, *b* presents optical microscope photos of the obtained powder particles. It is seen that the particles have an irregular shape with a wide range of sizes. The powder particles' average size was of ≅ 200 μm with observed variation from 4 to 380 μm. The size distribution curve of alloy powder particles is shown in Fig. 6.

Using the differential scanning calorimetry (DSC) method, it is shown that no phase transformations observed in the alloy powders in the temperature range up to the solidus temperature (Fig. 7). The observed solidus temperature is of ≅ 545–549°C, which is approximately of 10°C lower than the melting temperature of the (α-Al + Al_3Ni + Si) ternary eutectic in the Al–Si–Ni system [12]. Such solidus temperature lowing compared with the equilibrium phase diagram is in high accordance with the investigation and results from [3]. They explained the phenomenon by non-equilibrium intermetallics appearance during a rapid crystallization.

The alloys' CTE calculations were carried out by the dynamometric method for the initial (cast) state.

Figure 8 shows the experimental data of CTE measurement, and the calculation results are presented in Table 2. The obtained CTE values are quite close to steel ones, which are of ≅ $(11–15)\cdot10^{-6}$ K^{-1}.

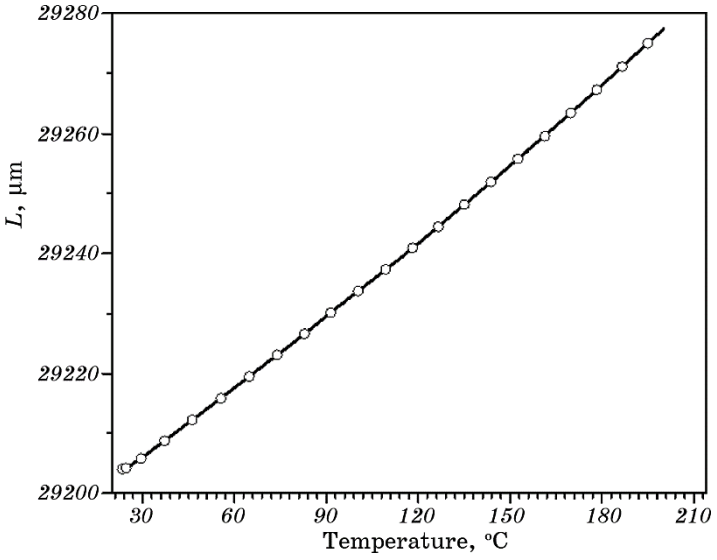

Fig. 8. The dynamometric curve of the studied alloy.

TABLE 2. The temperature dependence of the CTE.

Alloy	CTE, $10^6 \cdot K^{-1}$	
	100°C	200°C
Al (99.99)	23.43	24.92
Al–Si–Ni (cast alloy No. 3)	13.2	14.2

4. CONCLUSIONS

A technique was developed for pre-alloyed Al–Si–Ni powders manufacture. The proposed method consists of mechanical grinding of the rapidly-quenched (10^5–10^6 K/s) from the liquid state ribbons in a high-energy planetary ball mill for 30 minutes with a rotation frequency of 200 rpm and the mass of the balls to the mass of the powder ratio 10:1.

Using different methods of structural analysis, the phase composition and structure of the original cast aluminium alloy with ≅ 24–28% of Si and ≅ 5–7% of Ni and powders obtained by grinding in a high-energy ball mill of rapidly-quenched metal ribbons of such an alloy were studied.

The rapidly-quenched ribbons have two structural zones: a 15–20 μm homogeneous structure on the contact side adjacent to the barrel and a columnar structure with signs of fibrousness on the free side of the strip. No phase transformations were observed in the alloy powders in the temperature range up to the solidus temperature. It was found the solidus temperature declined compared with the equilibrium phase diagram to ≅ 545–549°C, which is ≅ 10°C lower. This shows that the structure obtained after the rapidly cooling solidification differs significantly from the equilibrium one.

It was established that the powders of these alloys have an irregular shape with a wide range of sizes from 4 to 500 μm, and the structure of the powders is optimal for further usage in powder metallurgy production.

REFERENCES

1. O. E. Osintsev, *Metal Sci. Heat Treatment*, **40**: 172 (1998).
2. *Aluminium Alloys: New Trends in Fabrication and Applications* (Ed. Zaki Ahmad) (Intechopen: 2012).
3. V. V. Vasenyev, *Razrabotka Kompozitsionnogo Materiala na Osnove Sistemy Al–Si–Ni s Nizkim Znacheniem TKLR i Tekhnologii Polucheniya Polufabrikatov dlya Izdeliy Raketno-Kosmicheskoy Tekhniki* [Development of a Composite Material Based on the Al–Ci–Ni System with a Low CTE Value and Technology for Producing Rocket and Space Technology Products] (Thesis of Disser. for Cand. Techn. Sci.) (Moskva: MAI: 2017) (in Russian).

4. Elwin L. Rooy, *Introduction to Aluminum and Aluminum Alloys* (ASM International: 1990).
5. O. E. Osintsev and S. L. Nikitin, *High-Strength Corrosion-Resistant Cast Aluminum Alloys of the Al–Mg System with a High Silicon Content* (MATI: 2008).
6. *Temperature Coefficient of Linear Expansion of Steel* (Online Resource) http://thermalinfo.ru/svojstva-materialov/metally-i-splavy/temperaturnyj-koeffitsient-linejnogo-rasshireniya-stali
7. G. V. Samsonov, *Handbook of the Physicochemical Properties of the Elements* (New York: Springer: 1968).
8. T. Bedo, B. Varga, D. Cristea, A. Nitoi, A. Gatto, E. Bassoli, G. Bulai, I.-L. Velicu, I. Ghiuta, S. Munteanu, M. A. Pop, C. Gabor, M. Cosnita, L. Parv, and D. Munteanu, *Metals*, **9**, Iss. 5: 483 (2019).
9. X. M. Pan, Z. P. Jin, and J. Zhao, *Metallurgical Mater. Trans. A*, **36**: 1757 (2005).
10. W. Xiong, Y. Du, R.-X. Hu, J. Wang, W.-W. Zhang, P. Nash, and X.-G. Lu, *Int. J. Mater. Research*, No. 6: 598 (2008).
11. N. A. Belov, S. V. Savchenko, and A. V. Khavan, *Fazovyy Sostav i Struktura Siluminov* [Phase Composition and Structure of Silumins] (MISiS: 2008) (in Russian).
12. V. S. Zolotorevsky, N. A. Belov, and M. V. Glazoff, *Casting Aluminum Alloys* (Amsterdam: Elsevier: 2007).